한국해양공학회 2003년도 추계학술대회 논문집 PP.226~231

자유표면 점성유동의 준쇄파 수치연구

곽승현*

한라대학교, 시스템응용공학부

Numerical Study on Sub-Breaking of Free Surface Viscous Flow

SEUNG-HYUN KWAG*

School of Applied System Engineering, Halla University

Key Words: Sub-Breaking Phenomena, Finite Difference Method, Triple Grid Scheme, Free Surface Flows, Catamaran Breaking Analysis

Abstract: *The viscous interaction of stern wave is studied by simulating the free-surface flows, including sub-breaking phenomena around a high speed catamaran hull advancing on calm water. The Navier-Stokes equation is solved by a finite difference method where the body-fittea coordinate system, the wall function and the triple-grid system are invoked. The numerical appearance of the sub-breaking waves is qualitatively supported by the experimental observation. They are also applied to study precisely on the stern flow of S-103 as to which extensive experimental data are available. For the catamaran, computations are carried out for the mono ana twin hulls.*

1. Introduction

Many studies have been performed on the wave breaking, for instance, Duncan(1993), Mori (1985), Grosenbaugh(1988), Maruo(1986). In spite of their extensive experiments, however, the free-surface nonlinear phenomena still remain unclear. Theoretical investigations are also attempted to explain the phenomena or to provide a suitable model. Dagan(1972) applied the instability analysis to predict the breaking.

The stern flows with the free-surface show also important phenomena in ship hydro-dynamics. Although Doi(1981) extensively studied about them, very little are made clear. Despite the viscous interactions are essential, theoretical approaches are so limited and most of the approaches are based on the simple flow models.

In the present study, the wave breaking and the viscous interaction of the stern waves are studied by making use of the results of numerical simulation. The numerical scheme for the simulation is based on the MAC method where the body-fitted coordinates and the non-staggered grid system are used. The convection terms are presented by the third-order upstream differencing.

2. Basic Equation and Numerical Scheme

Numerical simulations of 3-D free-surface flows are carried out by using the MAC method. The velocity components u, v and w at (n+1) time step are determined by

$$\begin{aligned} u^{n+1} &= (F^n - \Phi_x^n)\Delta t \\ v^{n+1} &= (G^n - \Phi_y^n)\Delta t \\ w^{n+1} &= (H^n - \Phi_z^n)\Delta t \end{aligned} \tag{1}$$

where

$$F^n = \frac{u^n}{\Delta t} + \left(\frac{1}{Re} + \upsilon_t\right)\nabla^2 u - \left(u^n\frac{\partial u}{\partial x} + v^n\frac{\partial u}{\partial y} + w^n\frac{\partial u}{\partial z}\right)$$

$$-\frac{\partial}{\partial x}\left\{ v_t\left(2\frac{\partial u}{\partial x}\right)\right\}-\frac{\partial}{\partial y}\left\{ v_t\left(\frac{\partial u}{\partial y}+\frac{\partial v}{\partial x}\right)\right\}$$
$$-\frac{\partial}{\partial z}\left\{ v_t\left(\frac{\partial u}{\partial z}+\frac{\partial w}{\partial x}\right)\right\}$$

$$G^n=\frac{v^n}{\triangle t}+\left(\frac{1}{Re}+v_t\right)\nabla^2 v$$
$$-\left(u^n\frac{\partial v}{\partial x}+v^n\frac{\partial v}{\partial y}+w^n\frac{\partial v}{\partial z}\right)$$
$$-\frac{\partial}{\partial x}\left\{ v_t\left(\frac{\partial u}{\partial y}+\frac{\partial v}{\partial x}\right)\right\}-\frac{\partial}{\partial y}\left\{ v_t\left(2\frac{\partial v}{\partial y}\right)\right\}$$
$$-\frac{\partial}{\partial z}\left\{ v_t\left(\frac{\partial v}{\partial z}+\frac{\partial w}{\partial y}\right)\right\} \qquad (2)$$

$$H^n=\frac{w^n}{\triangle t}+\left(\frac{1}{Re}+v_t\right)\nabla^2 w$$
$$-\left(u^n\frac{\partial w}{\partial x}+v^n\frac{\partial w}{\partial y}+w^n\frac{\partial w}{\partial z}\right)$$
$$-\frac{\partial}{\partial x}\left\{ v_t\left(\frac{\partial u}{\partial z}+\frac{\partial w}{\partial x}\right)\right\}-\frac{\partial}{\partial y}\left\{ v_t\left(\frac{\partial v}{\partial z}+\frac{\partial w}{\partial y}\right)\right\}$$
$$-\frac{\partial}{\partial z}\left\{ v_t\left(2\frac{\partial w}{\partial z}\right)\right\}$$

and

$$\Phi^n=p+\frac{z}{Fn^2} \qquad (3)$$

$$\nabla^2=\frac{\partial}{\partial x^2}+\frac{\partial}{\partial y^2}+\frac{\partial}{\partial z^2} \qquad (4)$$

Differentiating Eq. (1) with respect to x, y and z,

$$\nabla^2\Phi=F_x+G_y+H_z$$
$$-(u_x^{n+1}+v_y^{n+1}+w_z^{n+1})/\triangle t \qquad (5)$$

The last term in Eq. (5) is expected to be zero to satisfy the continuity condition. Eq. (5) can be solved by the relaxation method. The new free-surface at the (n+1)th time-step is calculated by moving the marker particles by

$$x^{n+1}=x^n+u^n\triangle t$$
$$y^{n+1}=y^n+v^n\triangle t \qquad (6)$$
$$z^{n+1}=z^n+w^n\triangle t$$

It is desirable to introduce coordinate transformations which simplify the computational domain in the transformed domain

$$\xi=\xi(x,y,z),\ \eta=\eta(x,y,z)$$
$$\zeta=\zeta(x,y,z) \qquad (7)$$

Through transformations, Eq. (1) can be written,

$$q_t+Uq_\xi+Vq_\eta+Wq_\zeta$$
$$=\left(\frac{1}{Re}+v_t\right)\nabla^2 q-K-REYSF(\xi,\eta,\zeta) \qquad (8)$$

where U, V and W are the contravariant velocities and K is the pressure gradient.

For the computation, three mesh systems are used whose sizes are different from each other depending on the characteristic of equations. It is called the TMM(triple mesh method). The first one is for the convective terms in the N-S equation, the second is for the Poisson equation, and the third is for the free-surface equation. The third grid system requires the finest one ; four times as large as the first one in the grid number at each direction. According to the results, the development of the free-surface elevation is strikingly improved. the CPU time and the memory size of the present computation are rather reduced owing to the use of coarse meshes of the second mesh system for the Poisson equation and the diffusion term (Xu, 1989). The grid size 74x29x19 is used for the TMM.

3. Detection of Sub-breaking Waves

3.1 Appearing Condition of Sub-breaking

The critical conditions for their appearance were studied in Mori(1989). There the breaking at their infant stage is concluded as a free-surface turbulent flow. The flow mechanism is supposed that the surplus energy accumulated around the wave crest by the increment of the free- surface could eventually maintain itself without any overturning or backward flows. An instability analysis provides a critical condition for their appearance;

$$\frac{M}{U_s}\frac{\partial M}{h\partial s}-\frac{1}{n_z}\frac{\partial n_z}{h\partial s}>0 \qquad (9)$$

where M is the circumferential force given by

$$M=(KU_s^2-n_zg)\,n_z \qquad (10)$$

s is the stream line coordinate along the free-surface and h is its metric coefficient, while n is the normal; n_z the direction cosine of n to z. U_s is the velocity component of basic flow in the s-direction; K is the curvature of the free-surface and g the gravity acceleration. Limiting ourselves to narrow proximity to the wave crest, we assume $n_z \fallingdotseq 1$ and $\partial/h\partial s \fallingdotseq \partial/\partial x$; then Eq. (9) can be reduced approximately into

$$\frac{U_s^2}{M}\frac{\partial}{\partial x}\frac{M}{U_s} > 0 \qquad (11)$$

where,

$$M = KU_s^2 - g \qquad (12)$$

Because M is always negative, the negative gradient of M/U_s to x suggests the possibilities for the free surface flow to be unstable. ζ is the free surface elevation.

3.2. Discussion on Stern Waves

The stern wave of S-103 is studied to make clear the flow mechanism especially on the viscous interaction by referring the computed results. S-103 ia an Inuid model with the beam/length ratio of 0.09 and extensive experiments have been carried out by Doi (1981). Fig. 1 shows the calculated and measured wave profiles along the hull surface at Fn=0.30. The computed profile shows a good agreement with the measured to conclude that the present numerical scheme works well and the results may endure for our purpose to discuss on the flow mechanism.

3.3 Discussion on Viscous Interaction

Fig. 2 shows the computed stern wave patterns at the three Froude numbers of 0.27, 0.28 and 0.30. Comparing the first stern wave crests, we can see that the result of Fn=0.27 looks different from the others; not so sharply developed. It differs from that of Fn=0.28 although the difference in the speed is not so large. The stern wave crest of Fn=0.27 is not clear. This may agree qualitatively with the observed. On the other hand, the crest of Fn=0.30 is rather sharp and large. The modest elevation of the stern wave at Fn=0.27 may be much related to the development of the boundary layer and separation.

3.4 Detection of Sub-Breaking

Fig. 3 shows the comparison of wave profiles and velocity vectors of Fn=0.30 between the measured (Doi,1981) and the calculated. The measured free-surface fluctuates intensively around the crest(indicated by I there). Because no special attention to the sub-breaking is paid in the calculation, the calculated free-surface is steady. It should be pointed out that the measured wave crest is in upstream compared with the calculated.

The detection of the appearance of sub-breaking waves is made for the stern waves at Fn=0.27 and 0.30. The values of M/U_s are calculated along y/l=0.09 which are shown in Fig. 4. A steep negative gradient is seen in Fn=0.30 but not so much in Fn=0.27. This means that the wave crest of Fn=0.30 can be subject to sub-breaking but not at Fn=0.27. It is concluded that the bow wave affects much on the separation and eventually the stern wave generation appreciably. The appearance of sub-breaking wave makes the flow field completely different and it may be necessary to include them in the computation.

3.5 Breaking Analysis of Catamaran

Steep negative gradient can be seen as the speed increases and the wave breaking can be serious at the large Froude number of 0.95. Fig. 5 and Fig. 6 show the breaking analysis for the mono and twin hulls at Fn=0.95. It is found that the breaking is much more serious in the case of catamaran rather than the mono hull, especially near the hull surface. Fig. 7 shows the photos for the stern waves at three speeds. Fig. 8 shows the wave height contours subject to the change of s/L. As the s/L becomes smaller, the divergent wave between the demihulls is eliminated and the transverse wave is dominant due to the wave interference.

4. Conclusions

(1) The criterion for the appearance of sub-breaking waves is numerically checked,

and the present numerical scheme can be applied to detect the occurrence of breaking waves of ships. The results are supported by the observation.

(2) The stern wave is much affected by the separation of the boundary layer flow which may be under the influence of the bow wave. The occurrence of sub-breaking changes the flow fields drastically, especially for the stern waves.

(3) The criterion is applied to the mono and twin hulls of catamaran. The breaking is more serious in the case of catamaran rather than the mono hull.

References

Dagan, G., Tulin, M. P., 1972, "Two Dimensional Free-Surface Gravity Flow past Blunt Bodies", Jour. Fluid Mech., Vol.51, Part3

Doi, Y., Kajitani, H., Miyata, H., Kuzumi, S., 1981, " Characteristics of Stern Waves generated by Ships of Simple Hull Form(1st Report)", Jour. of Soc. of Naval Arch. of Japan, Vol. 150

Duncan, J. H., 1993, "The Breaking and Non-breaking Wave Resistance of a Two-dimensional Hydrofoil", Jour. Fluid Mech., Vol. 126

Grosenbaugh, M. A., Yeung, R. W., 1988, "Non-linear Bow Flows - An Experimental and Theoretical Investigation", Proc. of 17th Symp. on Naval Hydro.

Maruo, H., Ikehata, M., 1986, "Some Discussions on the Free Surface Flow around the Bow", Proc. of 16th Symp. on Naval Hydro.

Mori, K., Doi, Y., 1985, "Flow Characteristics of 2-Dimensional Sub-Breaking Waves, turbulence Measurements and Flow Modeling", Hemisphere Pub. Co.

Mori, K., Shin, M. S., 1989, "Sub-Breaking Wave : Its Characteristics, Appearing Condition and Numerical Simulation", Proc. of 17th Symp. on Naval Hydro.

Xu, Q., Mori, K., Shin, M., 1989, "Double-Mesh Method for Efficient Finite-Difference Calculations", Jour. of the Soc. of Naval Arch. of Japan, Vol.166

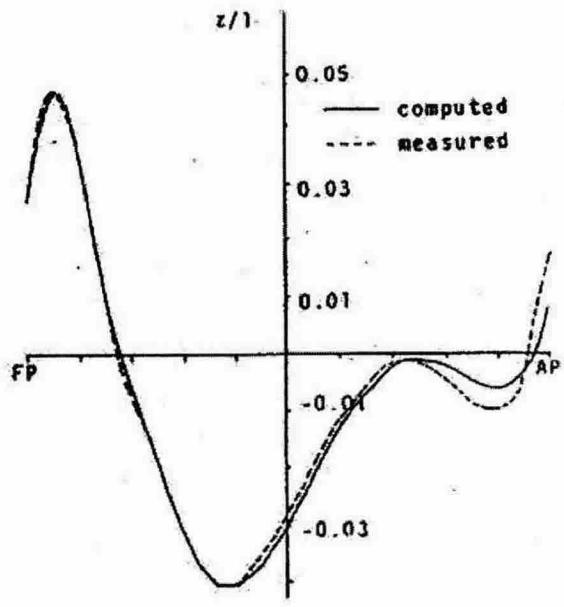

Fig. 1 Comparison of wave profile of S103

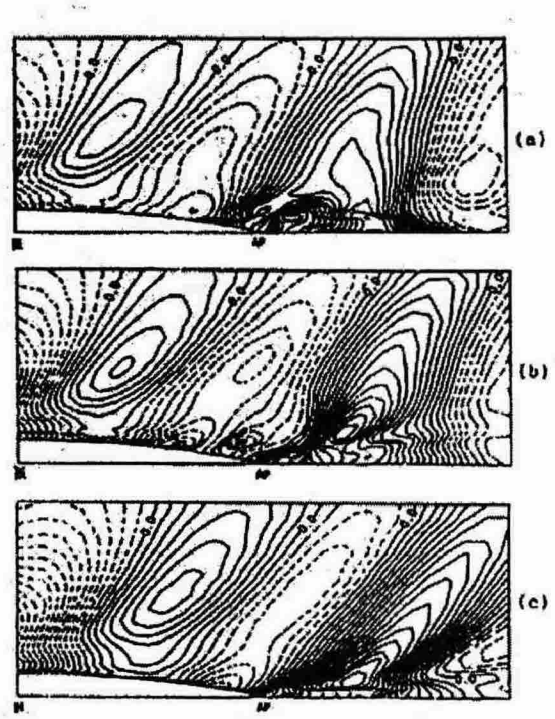

Fig. 2 Stern wave patterns of S103
(a) Fn=0.27 (b) 0.28 (c) 0.30
(Contour Interval 0.02 x $2g\zeta/U_0^2$)

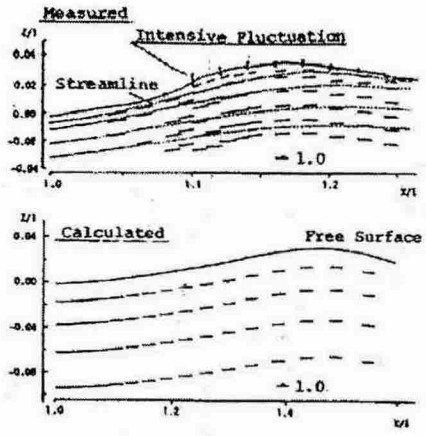

Fig. 3 Wave profile and velocity vector (x-z plane, y/l=0.15 for S103)

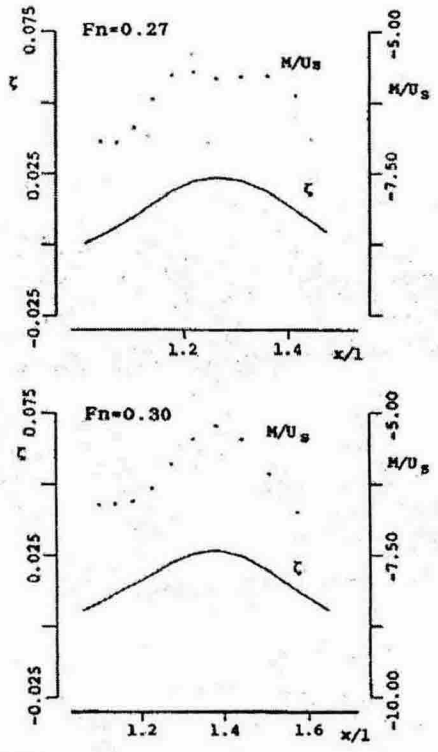

Fig. 4 Variation of M/U_S and free surface elevation and lines analysis of S103

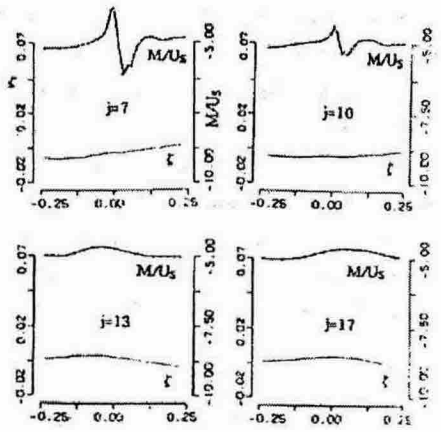

Fig. 5 Breaking analysis for mono hull ; M/U_S and free-surface amplitude

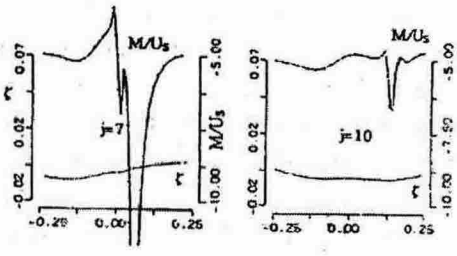

Fig. 6 Breaking analysis for twin hull ; M/U_S and free-surface amplitude

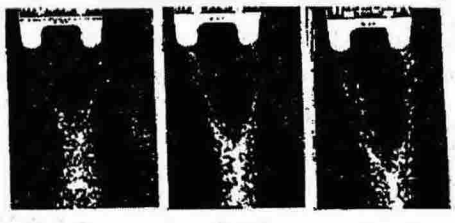

Fig. 7 Photos for stern waves of catamaran 4.0m/sec, 4.5m/sec, 5.0m/sec from l.h.s.

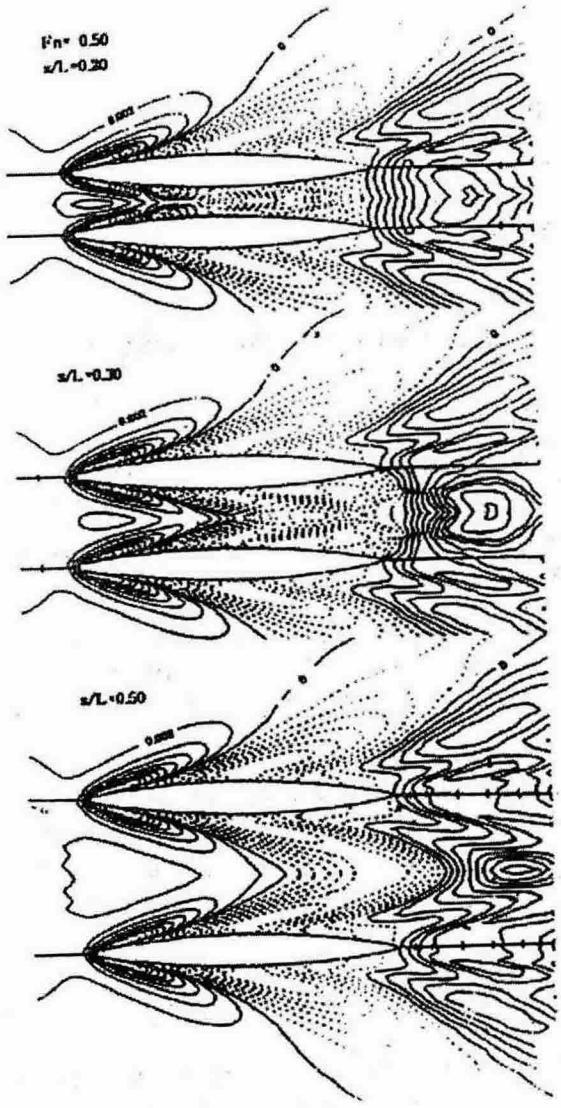

Fig. 8 Wave height contours at Fn=0.50
subject to s/L=0.20, 0.30, 0.50